

NUMERICAL SOLUTION OF THE SCHRÖDINGER EQUATION IN A WAVELET BASIS FOR HYDROGENLIKE ATOMS

PATRICK FISCHER* AND MIREILLE DEFRANCESCHI †

Abstract. An iterative method is proposed to solve the Schrödinger eigenvalue problem in a wavelet framework. Orthonormal wavelets are used to represent the corresponding operator as a sparse band matrix. This representation, called the Non Standard form, is obtained by means of the B.C.R. algorithm and brings simplifications in the numerical calculations. Problems due to the 1D mathematical model and to the discretization process receive special attention.

Key words. Wavelet decomposition, Schrödinger equation, iterative method.

AMS subject classifications. 42C15, 81Q05, 65F10.

1. Introduction. Most often, ab initio calculations in molecular quantum chemistry mean solving the time-independent Schrödinger equation $H\Psi_i = E_i\Psi_i$, where H is the Hamiltonian of the model molecular system, Ψ_i is the i^{th} wave function (stationary state), and E_i the corresponding eigenvalue [1]. However, except for a few simple systems, exact solutions to this equation are not accessible and therefore only approximate solutions are known. The mathematical difficulties due to the nature of the electrostatic interactions are such that explicit solutions for this problem are not obtainable even if its complexity is reduced by considering the motion of only the electrons in a fixed nuclear framework (Born-Oppenheimer approximation) [2].

Finding suitable but manageable approximate solutions to the electronic Schrödinger equation has thus been a major preoccupation of quantum chemists. The procedure most widely used to solve the equations consists in writing the molecular orbitals as a Linear Combination of Atomic Orbitals (LCAO approximation) which belong to a given complete set of the Sobolev space $H^1(\mathbb{R}^3)$. Computations with infinite bases are impracticable in actual calculations and, to obtain accurate results, truncated, but large basis set expansions are necessary. Because of computer limitations, these basis sets are rarely large enough to provide the required accuracy in molecules of chemical interest. The error resulting from this truncation is difficult to assess, and the way it affects the results largely depends on the physical properties under calculation.

Furthermore, within the traditional LCAO framework, basis sets have a tendency toward linear dependence as the size of the molecule increases. This is why, during the last three decades the finite element method has been explored to solve the Schrödinger equation. It has provided very accurate results to solve time-independent problems for simple systems [3, 4, 5, 6] or even time-dependent problems [7]. However there are two problems which prevent efficient application of the finite element method to large molecules. The first is the large storage requirement for the finite element matrices when extended to three dimensional systems. The second is to remove the singularities inherent to the nuclear potentials.

*Ceremade, Paris-Dauphine University, Pl. du Mal De Lattre de Tassigny, F75775, Paris Cedex 16, France (fischer@math.u-bordeaux.fr).

†CEA, DSM/DRECAM/SRSIM, CE-Saclay, F91191 Gif sur Yvette, France (defrancesc@basilic.cea.fr).

Recently, it was pointed out that this last restriction can be removed in momentum space (using a Fourier transform), and attempts to solve numerically the equations in momentum space have been reported for atoms, diatomic and polyatomic molecules, and even polymers [8, 9, 10, 11, 12].

However, this analysis, well known by chemists, can be usefully completed by using a wavelet transform. Results obtained by the authors with continuous wavelets to solve the Schrödinger equation for hydrogenlike atoms were considered promising enough to proceed further with investigations on wavelets in quantum chemistry [13, 14]. After this first work, it was natural to be interested by a matrix representation of operators in order to make numerical computations in a more efficient way (faster algorithms requiring less storage) than what can be done with finite element methods. This representation has been obtained by means of a decomposition of the Schrödinger operator onto an orthonormal wavelet basis [15].

The method of decomposition, first proposed by Beylkin, Coifman and Rokhlin (BCR) [16, 17], is based on the notion of multiresolution analysis [18, 19]. Orthonormal wavelets, constructed by Daubechies [20, 21] are used as basis functions to represent some operators. These wavelets are compactly supported and lead to sparse matrix representations. The study of the derivative and of the multiplicative (by a function) operators allows to analyze the Schrödinger equation whose wavelet transform is performed by sorting out the operator in two parts which are treated individually. The matrix coefficients corresponding to the kinetic term are given by an iterative process defined from relations existing between different scales and those related to the potential term are given by a quadrature formula constructed from a Taylor expansion of the integral kernel corresponding to the operator.

An iterative method for the solution of the hydrogenic Schrödinger equation, and using this particular matrix representation, is presented in this paper. Results obtained and problems related to the discretization are studied in details.

2. BCR Algorithm. Compactly supported wavelets with vanishing moments constructed by Daubechies are used in this work. These wavelets lead to band matrices with only few nonzero values around the main diagonal. The numerical evaluation of the corresponding coefficients is not described in this paper but can be found in [20, 21].

2.1. Wavelet decomposition of a function. We denote the scaling function by $\varphi(x)$ and the wavelet mother by $\psi(x)$. The corresponding wavelet bases are then given by:

$$(2.1) \quad \varphi_k^j(x) = 2^{-j/2} \varphi(2^{-j}x - k), \quad k, j \in \mathbb{Z},$$

$$(2.2) \quad \psi_k^j(x) = 2^{-j/2} \psi(2^{-j}x - k), \quad k, j \in \mathbb{Z}.$$

The wavelet mother corresponding to the chosen wavelet basis verifies:

$$(2.3) \quad \int_{\mathbb{R}} dx \psi(x) x^m = 0, \quad m = 0, \dots, M-1,$$

which means that it has M vanishing moments.

The scaling function $\varphi(x)$, and the wavelet mother $\psi(x)$ then verify the following scaling relations:

$$(2.4) \quad \varphi(x) = \sqrt{2} \sum_{k=0}^{L-1} h_k \varphi(2x - k), \quad h_k = \langle \varphi, \varphi_{-1,k} \rangle,$$

$$(2.5) \quad \psi(x) = \sqrt{2} \sum_{k=0}^{L-1} g_k \varphi(2x - k), \quad g_k = (-1)^k h_{L-k-1},$$

where the number L of coefficients is connected to the number M of vanishing moments and is also connected to other properties that can be imposed to $\varphi(x)$. Functions verifying (2.4) have their support included in $[0, \dots, L-1]$. Furthermore, if there exists a coarsest scale, $j = n$, and a finest one, $j = 0$, the bases can be rewritten as:

$$(2.6) \quad \varphi_{j,k}(x) = \sum_{l=0}^{L-1} h_l \varphi_{j-1,2k+l}(x), \quad j = 1, \dots, n,$$

and

$$(2.7) \quad \psi_{j,k}(x) = \sum_{l=0}^{L-1} g_l \varphi_{j-1,2k+l}(x), \quad j = 1, \dots, n.$$

The wavelet transform of a function $f(x)$ is then given by two sets of coefficients defined as

$$(2.8) \quad d_k^j = \int_{\mathbb{R}} dx f(x) \psi_{j,k}(x),$$

and

$$(2.9) \quad s_k^j = \int_{\mathbb{R}} dx f(x) \varphi_{j,k}(x).$$

Starting with an initial set of coefficients s_k^0 , and using (2.8) and (2.9), coefficients d_k^j and s_k^j can be computed by means of the following recursive relations:

$$(2.10) \quad d_k^j = \sum_{l=0}^{L-1} g_l s_{2k+l}^{j-1},$$

and

$$(2.11) \quad s_k^j = \sum_{l=0}^{L-1} h_l s_{2k+l}^{j-1}.$$

Coefficients d_k^j , and s_k^j are considered in (2.10) and (2.11) as periodic sequences with the period 2^{n-j} . The set d_k^j , is composed by coefficients corresponding to the decomposition of $f(x)$ on the basis $\psi_{j,k}$ and s_k^j may be interpreted as the set of averages between scales.

2.2. Non Standard form of integral operators. Let us consider operators that can be written in an integral form,

$$(2.12) \quad Tf(x) = \int_{\mathbb{R}} dy K(x,y) f(y),$$

where $K(x,y)$ is the integral kernel associated to the operator T . In order to carry out computations, the representation of an operator consists in writing the corresponding

kernel as a matrix. The Non Standard (NS) form related to a wavelet basis decomposition leads to sparse matrices and, as a result, speeds up calculations. It is obtained by developing the kernel on the following two dimensional basis:

$$(2.13) \quad \left\{ \psi_{j,k}(x) \psi_{j,k'}(y), \psi_{j,k}(x) \varphi_{j,k'}(y), \varphi_{j,k}(x) \psi_{j,k'}(y) \right\}_{j,k,k' \in \mathbb{Z}} .$$

Hence, the three sets of coefficients,

$$(2.14) \quad \alpha_{k,k'}^j = \iint_{\mathbb{R}^2} dx dy K(x, y) \psi_{j,k}(x) \psi_{j,k'}(y) ,$$

$$(2.15) \quad \beta_{k,k'}^j = \iint_{\mathbb{R}^2} dx dy K(x, y) \psi_{j,k}(x) \varphi_{j,k'}(y) ,$$

$$(2.16) \quad \gamma_{k,k'}^j = \iint_{\mathbb{R}^2} dx dy K(x, y) \varphi_{j,k}(x) \psi_{j,k'}(y) ,$$

have to be computed. By applying formulae (2.8) and (2.9), equations (2.14), (2.15), and (2.16) may be rewritten as:

$$(2.17) \quad \alpha_{k,k'}^j = \sum_{l,l'=0}^{L-1} g_l g_{l'} r_{2k+l,2k'+l'}^{j-1} ,$$

$$(2.18) \quad \beta_{k,k'}^j = \sum_{l,l'=0}^{L-1} g_l h_{l'} r_{2k+l,2k'+l'}^{j-1} ,$$

$$(2.19) \quad \gamma_{k,k'}^j = \sum_{l,l'=0}^{L-1} h_l g_{l'} r_{2k+l,2k'+l'}^{j-1} ,$$

where $r_{k,k'}^j$ is a fourth set of coefficients defined as,

$$(2.20) \quad r_{k,k'}^j = \iint_{\mathbb{R}^2} dx dy K(x, y) \varphi_{j,k}(x) \varphi_{j,k'}(y) ,$$

which verifies the recursive rule:

$$(2.21) \quad r_{k,k'}^j = \sum_{l,k'=0}^{L-1} h_l h_{l'} r_{2k+l,2k'+l'}^{j-1} ,$$

where $k, k' = 0, \dots, 2^{n-j} - 1, j = 1, \dots, n$.

If one denotes P_j the projection operator from $L^2(\mathbb{R})$ on the subspace spanned by the basis $\{\phi_{j,k}\}_{k \in \mathbb{Z}}$, and Q_j the projection operator on the subspace spanned by the basis $\{\psi_{j,k}\}_{k \in \mathbb{Z}}$, then $\{\alpha_{k,k'}^j\}_{k,k' \in \mathbb{Z}}$, $\{\beta_{k,k'}^j\}_{k,k' \in \mathbb{Z}}$, $\{\gamma_{k,k'}^j\}_{k,k' \in \mathbb{Z}}$, $\{r_{k,k'}^j\}_{k,k' \in \mathbb{Z}}$ represent the operators $A_j = Q_j T Q_j$, $B_j = Q_j T P_j$, $G_j = P_j T Q_j$, and $T_j = P_j T P_j$, respectively. The discretization T_0 of the operator T on the finest scale $j = 0$ may be written as:

$$(2.22) \quad T_0 = \sum_{j=1}^n A_j + B_j + G_j + T_n .$$

Using process (3.5), the ratio of two successive iterations leads to the highest eigenvalue. Although being similar, scheme (3.4) cannot be written as (3.5) because the matrix A_n in the process (3.4) changes at each iteration step. Furthermore, the goal of the computation is not to determine the lowest eigenvalue of A_n but the lowest one of the problem (3.3).

However, it is possible to obtain arguments about the convergence of (3.4) from the convergence of (3.5). Details about this result can be found in [28].

4. Implementation. The NS form given by the BCR algorithm is used to compute the matrix-vector products entering (3.4). The first step to obtain a NS form is to determine the coefficients corresponding to a discretization at the scale $j = 0$. The coefficients corresponding to the other scales can be obtained from these ones by using relations (2.10), (2.11), (2.17), (2.18), (2.19), and (2.21).

Both techniques described in [15] are used to build the NS decomposition corresponding to the operator,

$$(4.1) \quad \frac{\Delta}{2} + \varepsilon^{(n)} .$$

This matrix is then inverted and the result is also expressed in a NS form. A quadrature formula is used to determine the decompositions of the potential term and of $f^{(n)}(x)$, and their NS forms are used to compute their product (the result is reconstructed and decomposed in a NS form). The result of the last product between the inverse matrix and $Zf^{(n)}/|x|$ is then reconstructed. The corresponding energy is computed to estimate the convergence of the process and to be used at the next iteration step. A test to stop the process is introduced after the energy evaluation.

The various calculations which have to be done to perform one iteration of the process can be summarized as follows:

1. Determination of the NS form of $\frac{\Delta}{2} + \varepsilon^{(n)}$.
2. Inversion of the matrix of $\frac{\Delta}{2} + \varepsilon^{(n)}$ using its NS decomposition.
3. Determination of the NS form of $\frac{Z}{|x|}$.
4. Determination of the NS form of $f^{(n)}(x)$.
5. Multiplication of result 4 by result 3: $\frac{Z}{|x|}f^{(n)}(x)$.
6. Reconstruction and determination of the NS form of result 5.
7. Multiplication of result 2 by result 6: $(\frac{\Delta}{2} + \varepsilon^{(n)})^{-1} \frac{Z}{|x|}f^{(n)}(x)$.
8. Reconstruction and determination of the NS form of result 7.
9. Computation of the energy from the function obtained in 8.

In fact, steps 3, 4, 5 and 6, performed during the computation of step 9 of iteration $n - 1$, are essential intermediate steps to determine the contribution of the potential term in the total energy at iteration n . In practice, it is sufficient to store the vector corresponding to the NS form of the potential term from one iteration to the next one.

These various steps require $O(N)$ operations (using the quadrature formula at step 3). The inversion in step 2 is performed by using the Schultz method, with a fast matrix multiplication algorithm [9]. The inverse, namely the operator A_n , is symmetric and the corresponding matrix representation is sparse. In particular, it can be specified that 29% of the coefficients are greater than 10^{-14} and only 11% are greater than 10^{-6} (localized in a band structure around the main diagonal). The sparsity of the representation of the wave function itself is quite fussy to assess since it depends on the discretization step size. Indeed, for a given number of discretization points,

it has already been shown in [15] that the accuracy can be significantly improved by reducing the size of the discretization interval (leading also to a dense representation). Using this trick, a compromise between the sparsity and the accuracy has to be done. The importance of the discretization step size is emphasized in the next part.

5. Applications. The number L of coefficients $\{h_k\}$ is equal to $3M$, and the results presented in the sequel have been obtained with $M = 4$. The results do not present significant differences with those obtained with $M = 6$. The program has been run for several values of N (number of discretization points), and the results given in this paper correspond to $N = 256$. It will be shown in the sequel that the size of the discretization step is a determining factor for the convergence of the process.

The graphs of the evolution of the energy with the number of iterations for two values of the nucleus charge Z ($Z = 1, 2$) are shown in Figs. 5.1 and 5.2. These figures show the first 30 iterations, and have been obtained with a size of discretization step leading to the best total energy for the initial function, i.e. a single optimized Gaussian function.

In both cases a first convergence plateau around the theoretical expectation value is followed by a strong energy decrease. Then, another convergence regime sets up around a second plateau located at a much lower energy value than the first one. The problem is then to give a physical interpretation of this second plateau.

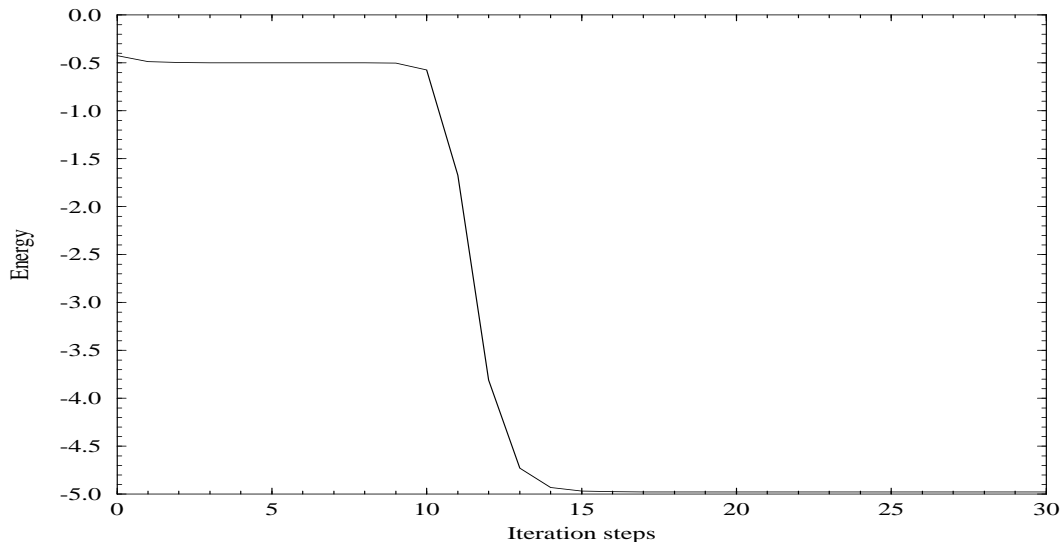


FIG. 5.1. *Evolution of the energy with the number of iterations; H : $Z = 1$.*

5.1. Mathematical origin of the second plateau. This phenomenon has its origin in the use of a quadrature formula to determine the NS form of the potential term which transforms the Coulombic singularity into a “pseudo-potential” without singularity. Hence, the second plateau corresponds exactly to the real ground state related to this pseudo-potential [29].

This hypothesis is verified by modifying the pseudo-potential in order to follow the behavior of the second plateau. This is done by changing the size of the discretization

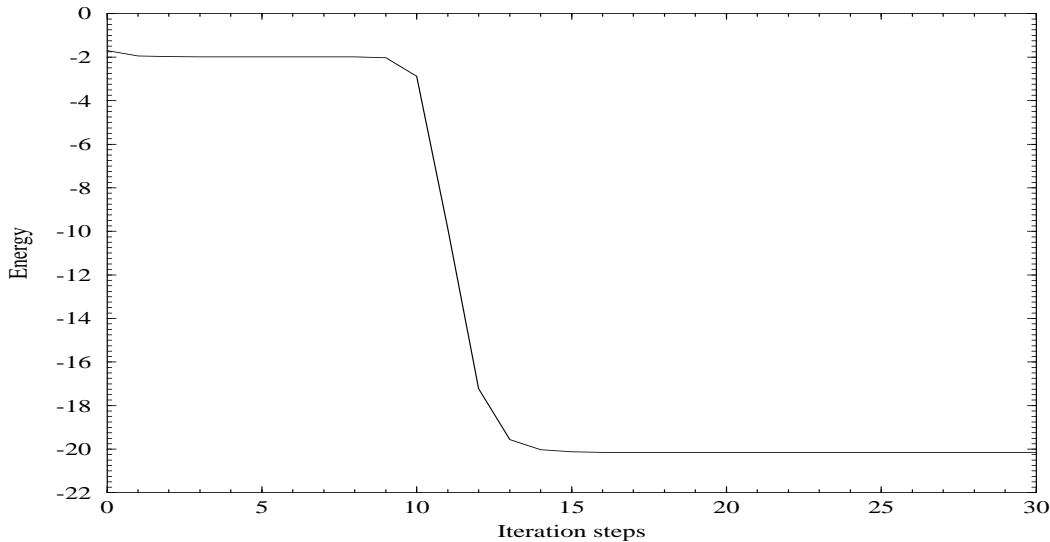


FIG. 5.2. *Evolution of the energy with the number of iterations; $He^+ : Z = 2$.*

step. In order to keep a good accuracy in the results, the number of discretization points is kept equal to 256, but the size of the interval is modified. The graphs corresponding to various sizes of interval are shown in Fig. 5.3 for the case $Z = 1$ (the same analysis can be done for other values of $Z, Z > 0$).

It can be noticed that the first plateau remains located around the exact energy value for the ground state of H and He^+ ($\varepsilon = -0.5$ for H , and $\varepsilon = -2.0$ for He^+) while the value of the second strongly depends on the point density.

The energy values achieved on the first plateau for the various discretization step sizes are summarized in the table 1, and can be compared to the theoretical energy. It can be noticed that the best initial interval size does not lead to the best accuracy after the convergence. This can be easily explained by the fact that the exact solution (i.e. the so-called Slater function) is wider than the initial function.

As expected, to a higher density of points corresponds a deeper pseudo-potential with a lower ground state. In the limit, the singular potential would be restored and the ground state would have a negative infinite energy [29]. However, this ground state does not correspond to a physically acceptable state for hydrogenlike atoms. Indeed, it will be outlined in the sequel that the corresponding probability density is a delta function $\delta(x)$.

5.2. Physical admissibility of the solutions. The evolution of the wave function itself instead of the energy is studied in this part. The graphs of the initial function, the 11th iterate (first plateau of convergence) and the exact solution of the problem are shown in Fig. 5.4. It must be born in mind that, due to condition (3.2), functions are antisymmetric by construction.

It is obvious from Fig. 5.4 that to the first energy plateau corresponds a real convergence towards the exact solution. Furthermore, Fig. 5.5 shows that the next iterations distort the function and lead to a symmetrical behavior which is reminiscent of a delta function. This function is exactly the ground state corresponding to the

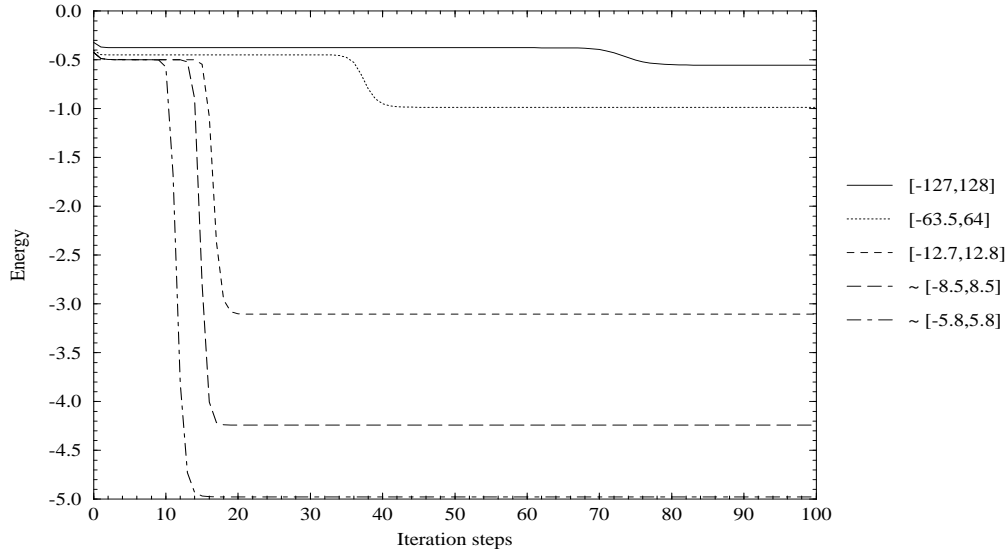


FIG. 5.3. Evolution of the energy with the number of iterations for various intervals; atom $H(Z = 1)$.

TABLE 5.1

Energy values for the initial function and for the function achieved on the first plateau for various interval sizes.

	[-127:128]	[-63.5:64]	[-12.7:12.8]	[-8.5:8.5]	[-5.8:5.8]
$\varepsilon^{(0)}$	-0.3199111	-0.4034546	-0.4236139	-0.4240615	-0.4242511
Error	$3.60 \cdot 10^{-1}$	$1.93 \cdot 10^{-1}$	$1.53 \cdot 10^{-1}$	$1.52 \cdot 10^{-1}$	$1.51 \cdot 10^{-1}$
$\varepsilon^{(n)}$	-0.3757223	-0.4484342	-0.4969135	-0.4985831	-0.4983637
Error	$2.49 \cdot 10^{-1}$	$1.03 \cdot 10^{-1}$	$6.17 \cdot 10^{-3}$	$2.83 \cdot 10^{-3}$	$3.27 \cdot 10^{-3}$

pseudo-potential, but it does not verify the condition of physical admissibility (3.2).

This analysis points to the fact that the second plateau observed in Fig. 5.1 (or in Fig. 5.2) corresponds to a “mathematical” solution of the 1D discretized problem. A possible way to avoid this undesired solution is to constrain the antisymmetry of the wave function at each iteration step. This can be easily achieved by means of the

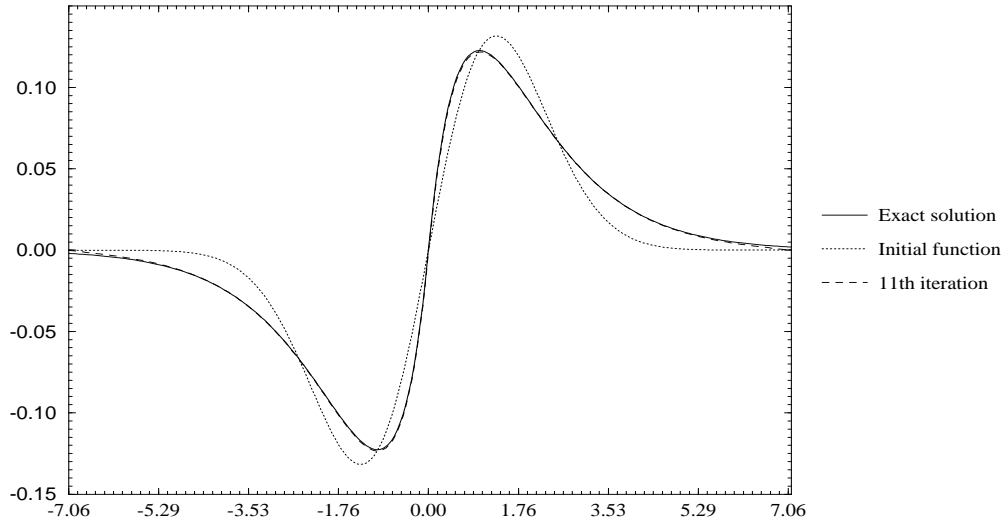


FIG. 5.4. *Graphs of various functions: initial function, 11th iteration and exact solution.*

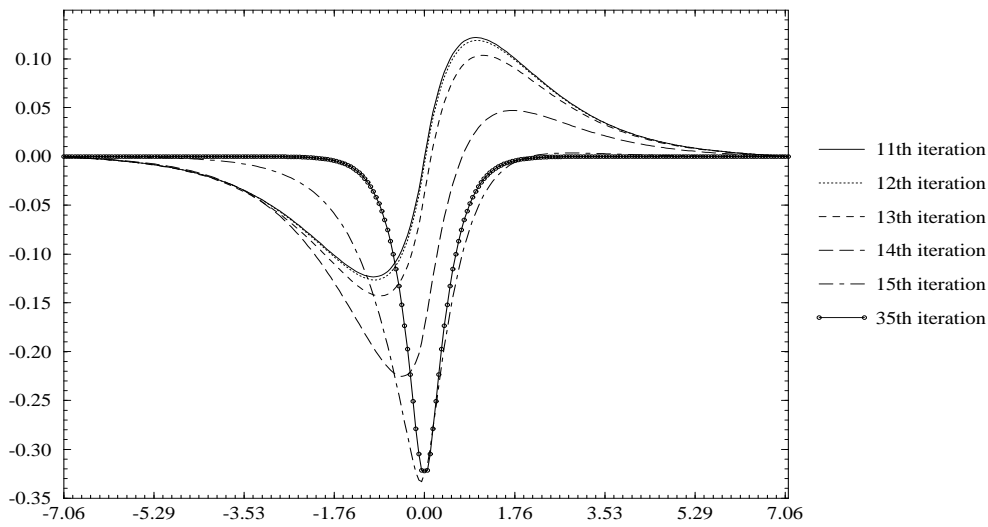


FIG. 5.5. *Graphs of various functions: 11th iteration, 12th iteration, 13th iteration, 14th iteration, 15th iteration and 35th iteration.*

following computational device:

$$(5.1) \quad f(x_i)_n = \frac{f(x_i)_0 - f(-x_i)_0}{2},$$

with $f(x_i)_0$: value of f in x_i before antisymmetrization,
 $f(x_i)_n$: value of f in x_i after antisymmetrization.

The physical ground state of the initial 3D problem can thus be obtained by using the iterative method equipped with this antisymmetry requirement. It suffices to divide the positive part of the result by x to obtain the radial behavior of the exact 3D wave function corresponding to the ground state.

6. Conclusion. In this work, we have used orthonormal wavelets to decompose the Schrödinger operator in a NS form. This particular representation has been used in an iterative method to solve the corresponding eigenvalue problem for hydrogenlike atoms. Results have shown that this method is really suited to this kind of problem. In particular, it has been shown that a particular attention is required when mathematical or numerical models are used to approximate a solution. This work opens the prospect of applying wavelets to study polyatomic and extended systems which are of interest to chemists.

Wavelets, mainly used in signal analysis are expected to be of interest in chemistry and in physics. This work, and others [30, 31], show that wavelet-based methods have a real promise to help solving physical problems.

Acknowledgements. The authors thank J. Delhalle and A. Cohen for many stimulating discussions and for reading the manuscript, and they greatly acknowledge the referee and G. Beylkin for most valuable comments. This work has been supported in part within the Tournesol Exchange Agreement No. 94-040 between the Communauté Française de Belgique and France.

REFERENCES

- [1] R. Mc Weeny, *Methods of molecular quantum mechanics*, Academic Press, 2nd ed., New York, 1989.
- [2] A. Szabo, N.S. Ostlund, *Modern quantum chemistry*, Mc Millan, New York, 1982.
- [3] D. Sundholm, J. Olsen, *Large MCHF calculations on the electron affinity of boron*, Chem. Phys. Letters **171**, (1990), pp. 53-57.
- [4] D. Sundholm, J. Olsen, *Finite element multiconfiguration Hartree-Fock calculations of the atomic quadrupole moments of excited states of Be, Al, In, Ne, Ar, Kr, and Xe*, Phys. Rev. **A47**, (1993), pp. 2672-2679.
- [5] S. Hackel, D. Heinemann, D. Kolb, B. Fricke, *Calculations of the polycentric linear molecule H_3^{2+} with the finite element method*, Chem. Phys. Letters **206**, (1993), pp. 91-95.
- [6] H. Murakami, V. Sonnad, E. Clementi, *A three-dimensional finite element approach towards molecular SCF computations*, Intern. J. Quantum Chem. **42**, (1992), pp. 785-817.
- [7] A.D. Bandrauk, *Molecules in laser fields*, Marcel Dekker, New York, 1993.
- [8] P. Fischer, M. Defranceschi, J. Delhalle, *Molecular Hartree-Fock equations for iteration-variation calculations in momentum space*, J. Numer. Math. **63**, (1992), pp. 67-82.
- [9] P. Fischer, L. De Windt, M. Defranceschi, J. Delhalle, *Electronic structure of H_2 and HeH^+ computed directly in momentum space*, J. Chem. Phys. **99** (10), (1993), pp. 7888-7898.
- [10] L. Dewindt, M. Defranceschi, J. Delhalle, *Electronic structure of Li^- and F^- calculated directly in momentum space*, J. Theor. Chem. Acta **86**, (1993), pp. 487-496.
- [11] J. Navaza, G. Tsoucaris, *Molecular wave functions in momentum space*, Phys. Rev. **A24**, (1981), pp. 683-692.
- [12] *Numerical determination of the electronic structure of atoms, diatomics, and polyatomic molecules*, edited by M. Defranceschi and J. Delhalle, NATO ASI, Vol. C271, Kluwer Academic, Dordrecht, 1989.
- [13] P. Fischer, M. Defranceschi, *Looking at atomic orbitals through Fourier and wavelet transforms*, Int. J. Quant. Chem. **45**, (1993), pp. 619-636.
- [14] P. Fischer, M. Defranceschi, *Iterative process for solving Hartree-Fock equations by means of a wavelet transform*, Appl. Comput. Harm. Anal. **1**, (1994), pp. 232-241.
- [15] P. Fischer, M. Defranceschi, *Representation of the atomic Hartree-Fock equations in a wavelet basis by means of the BCR algorithm*, in: Wavelets: Theory, Algorithms, and Applications. (C.K. Chui, L. Montefusco, L. Puccio, Eds.), Academic Press Inc, 1994, pp. 495-506.

- [16] G. Beylkin, R. Coifman, V. Rokhlin, *Fast wavelet transforms and numerical algorithms I*, Comm. Pure Appl. Math. **44**, (1991), pp. 141-183.
- [17] G. Beylkin, *Wavelets, multiresolution analysis and fast numerical algorithms*, a draft of INRIA lecture notes (1991).
- [18] T.H. Koornwinder, *Fast wavelet transforms and Calderon-Zygmund operators*, in Wavelets: An Elementary Treatment of Theory and Applications, Koornwinder, T.H., Ed, World Scientific Publishing Co, Amsterdam, 1993, pp. 161-182.
- [19] S. Mallat, *Multiresolution approximations and wavelet orthogonal bases of $L^2(\mathbb{R})$* , Trans. Am. Math. Soc. **315**, (1989), pp. 69-87.
- [20] I. Daubechies, *Orthonormal bases of compactly supported wavelets*, Comm. Pure Appl. Math. **41**, (1988), pp. 909-996.
- [21] I. Daubechies, *Ten lectures on wavelets*, CBMS 61, SIAM, Philadelphia, 1992.
- [22] T.F. Jordan, *Conditions on wave functions derived from operator domains*, Am. J. Phys. **44**, (1976), pp. 567-570.
- [23] C. Cohen-Tannoudji, B. Diu, F. Laloe, *Mécanique Quantique*, vol. I, Hermann, Paris, 1982.
- [24] T. Koga, A.J. Thakkar, *Linear integrability of wave functions*, Int. J. Quant. Chem. **34**, (1988), pp. 103-106.
- [25] H.Y. Pan, Z.S. Zhao, *On the conditions for physical admissibility of Schrödinger wave functions*, Int. J. Quant. Chem. **40**, (1991), pp. 605-609.
- [26] P. Lascaux, R. Theodor, *Analyse numérique matricielle appliquée à l'art de l'ingénieur*, II, Masson, Paris, 1987.
- [27] F. Chatelin, *Valeurs propres de matrices*, Masson, Paris, 1988.
- [28] P. Fischer, Thesis of the Paris-Dauphine University, 1994.
- [29] R. Loudon, *One-dimensional hydrogen atom*, Am. J. Phys. **27**, (1959), pp. 649-655.
- [30] K. Cho, A. Arias, J.D. Joannopoulos, P.K. Lam, *Wavelets in electronic structure calculations*, Phys. Rev. Lett. **71**, (1993), pp. 1808-1811.
- [31] J.P. Antoine, F. Bagarello, *Wavelet-like orthonormal bases for the lowest Landau level*, J. Phys. **A27**, (1994), pp. 2471-2481.